ORIGINAL ARTICLE

Parametric studies on the CO_2 laser cutting of Kevlar-49 composite

T. A. El-Taweel · A. M. Abdel-Maaboud · B. S. Azzam ·
A. E. Mohammad

Abstract In the present study, the cutting performance of a
CO_2 laser on Kevlar-49 composite materials has been
studied. The Taguchi technique is employed to identify the
effect of laser control parameters, i.e., laser power, cutting
speed, material thickness, assistance gas pressure, and laser
mode, on the quality of cut parameters, namely, kerf width,
dross height, and slope of the cut. From the analysis of
variance (ANOVA) and signal-to-noise (S/N) ratio response
tables, the significant parameters and the optimal combina-
tion levels of cutting parameters are determined. The
obtained results are interpreted and modeled to closely
understand the behavior and quality of CO_2 laser cutting.
Kevlar-49 composites are found to be cut satisfactorily by
the CO_2 laser at the optimum process parameter ranges. The
results showed that laser power is the most significant
parameter affecting the quality of cut parameters. The
optimal combination of cutting parameters minimized the
kerf width, dross height, and slope of cut to 0.103 mm,
0.101 mm, and 2.06°, respectively. The error between
experimental results with optimum settings and the pre-
dicted values for the kerf width, dross height, and slope of
cut lie within 2.9%, 7.92%, and 6.3%, respectively.

T. A. El-Taweel (✉) · A. M. Abdel-Maaboud
Department of Production Engineering & Mechanical Design,
Faculty of Engineering, Menoufia University,
Gamal abd Elnaser Street,
Shebin-El-Kom 01254, Egypt
e-mail: tahaeltaweel@yahoo.com

B. S. Azzam
Faculty of Engineering, Cairo University,
Cairo, Egypt

A. E. Mohammad
NILES, Cairo University,
Cairo, Egypt

Abbreviations

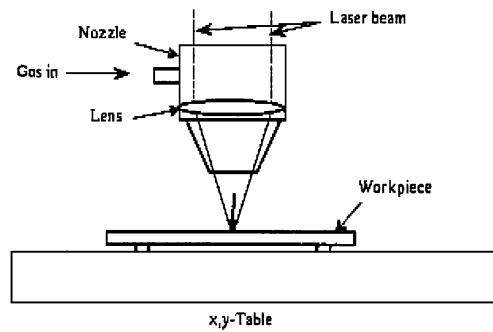|	
CW	continuous wave mode
D	dross height (mm)
KW	mean value of kerf width (mm)
k	number of control parameters
L_{in}	kerf width in the laser input surface (mm)
L_{out}	kerf width in the laser output surface (mm)
M	laser mode
S	slope of cut (°)
T	workpiece thickness (mm)
α	slope angle (°)
P	laser power (W)
Pr	assistance gas pressure (bar)
P1	gated pulse mode
P2	super pulse mode
P3	hyper pulse mode
V	cutting speed (m/min)
y_i	response value in the ith experimental run
η	signal-to-noise (S/N) ratio (dB)
$\overline{\eta}$	overall mean value of the S/N ratio for all experi-mental runs (dB)
η_{mi}	average S/N ratio for the ith control parameter (dB)
η_{opt}	predicted S/N ratio at the optimum parameter levels (dB)

1 Introduction

Considerable research in the field of material science has
been directed towards the development of new light-weight,

Table 1 Typical properties of Kevlar-49 [1]

Properties	Description
Fiber material	Kevlar-49
Density (g/cm^3)	1.45
Parallel to fibers	125
Tensile strength (GPa)	2.8–3.5
Strain to fracture (%)	2.2–2.8
Parallel to fibers	−5 to −2
Perpendicular to fibers	60

Fig. 2 Schematic of the experimental setup

high-performance engineering materials, such as composites. Fiber-reinforced composite materials are one of the most widely used materials for structural applications, particularly for aerospace structures and the military industry. Properties such as high specific strength, specific stiffness, and ease of tailoring to a specific need make them attractive [1]. Kevlar-49 is the commercial name of a polytropic liquid crystalline aromatic polyamide. It consists of long molecular chains produced from poly paraphenylene terephthalamide. The chains are highly oriented with strong inter-chain bonding, which result in a unique combination of properties. It is five times stronger than steel on an equal weight basis as a result of the strong covalent bonding in the fiber direction and weak hydrogen bonding in the transverse direction in highly anisotropic properties of Kevlar-49 fiber [1, 2]. Kevlar fibers can resist reasonably high temperatures and corrosion. It is very versatile fiber and has been used for interior panels and structural aircraft parts, facings for automobile clutch plates, for belts in tires, cut-resistant and bullet-proof clothing for military and police use, and in combination with other fibers in boat hulls, skis, and pressure vessels [3]. However, the machining of fiber-reinforced composites by conventional cutting tools is difficult and results in poor cut quality. This is mainly because of inhomogeneous composition, anisotropy, and excessive frictional force

developed on the cutting tool due to thermal expansion. In addition, the delamination and fiber spalling from the cut edges significantly reduce the final product quality [4–6].

Laser cutting, being a non-contact process, does not involve any mechanical cutting forces or tool wear. However, as laser cutting is based on the interaction of a laser beam with the composites, defects that are thermal in origin may arise if proper care is not taken regarding the selection of the cutting parameters ranges. Applications of laser beams in modern industries are increasing at a fast pace due to their ability to cut either very hard or very soft materials, electrically conductive as well as non-conductive materials, such as high-strength steel (HSS), ceramics, composites, diamond, plastics, and rubber. The literature available so far suggest that lasers can be very useful in the machining of composite materials [7–14].

Yilbas [15] studied the laser cutting of composite materials and indicated that the cut quality could be improved by the proper setting of laser parameters. Al-Sulaiman et al. [16] investigated the laser cutting of carbon-reinforced carbon laminate. They showed that the cutting quality improves at a certain range of laser parameters. Another work by Al-Sulaiman and Yilbas [17] investigated the laser drilling of composite and metallic materials, and showed that the specific energy required for laser drilling was lower than that of the conventional drilling method.
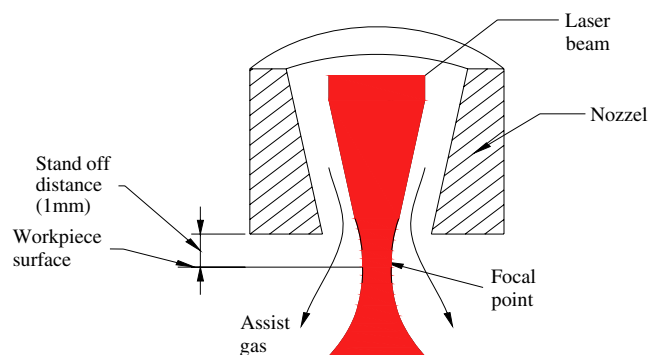

Fig. 1 The CO_2 laser cutting machine utilized in this study

Fig. 3 Schematic of the laser's focal point position

Table 2 Laser cutting conditions

Working parameters	Description
Laser power (W)	800–2,000
Speed (m/min)	7.5–30
Material thickness (mm)	1–10
Gas pressure (bar)	3–16
Laser mode	CW, P1, P2, P3
Lens focal length (mm)	100
Stand-off space (mm)	1
Nozzle diameter (mm)	0.8
Assistance gas type	Nitrogen

The drilling process was modeled based on the material removal over the diameter of the hole drilled. They showed that large-diameter drilling can be achieved through the cutting of the substrate material, which lowers the specific energy required when producing the hole. Al-Sulaiman et al. [18] carried out hole cutting into Kevlar laminates with different thicknesses and properties using a CO_2 laser. They observed that the damage size is significantly affected by the laser-irradiated power. Laser drilling in Kevlar and glass/epoxy composites for multi-layer printed boards were investigated by Hirogaki et al. [19]. They demonstrated that the surface roughness of the holes drilled in Kevlar was smaller than that of holes drilled in glass/epoxy composite. Ilio and Tagliaferri [20] showed that thermally induced cracks were developed in plies with the fiber direction at 90° to the cutting direction. The material properties and laser cutting of composites were also examined by Chen and Cheng [7], who developed a heat-transfer model to determine the relative heat-affected zones of the composites and indicated that Kevlar composites could be cut smoothly, while graphite composites were difficult to cut. The laser cutting of Kevlar and chemical by-products was studied by Doyle and Kokosa [21], who showed that the chemical products were toxic and that care should be taken the during the laser processing of Kevlar.

According to the above arguments, several studies on how laser control parameters affect the cutting quality were reported. However, its application to Kevlar-49 has not been considered in the previous literature. Therefore, it is imperative to develop a suitable technology guideline for the optimum cutting parameters of Kevlar-49 composites. In the present work, the variation of kerf width (KW), dross height (D), and the slope of cut (S) with the laser cutting parameters, such as power (P), speed (V), material thickness (T), assistance gas pressure (Pr), and laser mode (M) was determined. Through the Taguchi technique, optimization of the cutting parameters for minimum kerf width, dross height, and the slope of cut has been also investigated.
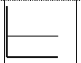
2 Experimental details

2.1 Material preparation

In this study, Kevlar-49 composite material was used as the workpiece in plate form. This material was chosen because of its wide range of application in the industry (such as automotive, aircrafts, boats, sports, and bullet-proof clothing for military and police use). Furthermore, this composite is very difficult to be cut by traditional cutting techniques [4, 12]. Kevlar-49 composite plate specimens fabricated from Kevlar-49 fibers were procured and received from the local market. The Kevlar-49-reinforced specimens have been examined under static and impact loads to measure their mechanical properties and to assess their behavior. Table 1 lists the typical properties of Kevlar-49. The specimens are Kevlar-49 woven-fabric cloth with a simple cloth and a simple orthogonal weave. The plate specimens are ordered in four lay-up forms, $[0°/90°]_2$ and $[\pm45°]_2$, which contain two woven mats, and $[0°/90°]_4$ and $[\pm45°]_4$, which contain four woven mats. The panels are flat and do not show any warping. Neither visible surface defects nor edge delamination are present. The orientation of the fibers is consistent with the specified lay-up. The density of the composite was about 1.45 g/cm^3 [1].

2.2 Experimental procedure

The experiments were carried out using a Prima Optimo 5-axis (England) CO_2 laser cutting machine. Figure 1 shows the utilized CO_2 laser cutting machine. The

Table 3 Operating laser modes

Description	Beam off	CW	Gated pulse (P1)	Super pulse (P2)	Hyper pulse (P3)
Beam on control	0	1	1	1	1
Pulse pin 5	X	0	1	1	0
Enhanced pulse pin 6	X	0	0	1	1
Beam profile					

Fig. 4 Geometry of the laser cut

and ±0.002-mm accuracy. The slope angle of the cut (α) was calculated using the following formula:

$$\alpha = \tan^{-1} \frac{\left(\frac{L_{in} - L_{out}}{2} \right)}{T} \; (^\circ) \tag{2}$$

where:

L_{in} Kerf width in the laser input surface (mm)
L_{out} Kerf width in the laser output surface (mm)
T Workpiece thickness (mm)

2.3 Preliminary experiments

Through the review of previous experience and literature surveys [18–24], it was found that choosing a control parameter either too large or too small may cause the degradation of cutting qualities. To identify the appropriate range for each control parameter, some preliminary experiments must be conducted to determine the acceptable lower and upper bounds. Preliminary experiments are helpful in shortening the allowable ranges of control parameters and in reducing the number of matrix experiments. The first experiment, which tests the cutting ability by adopting a low laser power, employs laser parameters having a laser power of 400 W and a cutting speed of 5 m/min. The second experiment, which tests the cutting ability by adopting a high laser power, employs laser parameters of 2,000 W and a cutting speed of 35 m/min. The photographs in Fig. 5 show the cutting results of the two experiments. It can be observed that the first experiment adopting a lower laser power yields inhomogeneous cutting with excessive widths of the cutting line. On the other hand, the second experiment adopting a higher laser power and cutting speed yields over-cutting and a heat-affected zone (HAZ). It should be noted that the effect of the laser power on the damaged size is found to be significant, which is attributed to the oxidation reactions taking place locally at high laser power levels. Delamination and loose fibers from the cut edges are not observed in laser-cut sides, while it is the opposite for the conventional cutting method.
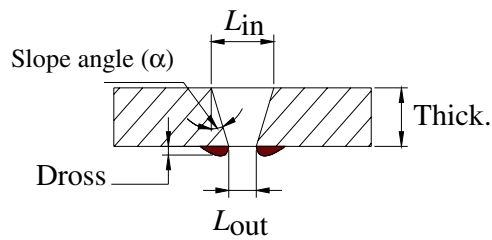
schematic of the experimental setup is shown in Fig. 2. The laser generator unit is a CO_2 Slab-laser model Rofin-Sinar DC 25. The gas discharge is created between two RF-excited electrodes. The resultant beam profile of the generator is of 001 mode, and it forms a beam print on a piece of transparent acrylic; the resulting profile shows a Gaussian beam profile that is suitable for cutting applications. The optical path of the Optimo machine includes seven flat mirrors, three fixed and four moving with machine carriages and rotating axes. The mirrors guide the laser beam from the laser generator up to the focusing lens and onto the workpiece. Figure 3 represents a schematic of the laser's focal point position. Table 2 lists the used laser cutting conditions. Four laser modes were used in the cutting process, namely, continuous wave (CW), gated pulse (P1), super pulse (P2), and hyper pulse (P3). Table 3 presents the applied operating laser modes.

Figure 4 shows the geometry of the laser cut. According to the DIN standard EN ISO 9013:2000 [22], the lower kerf width was measured using a Nikon model V-16B 10× type profile projector, while the upper kerf width was measured using a filler gauge. The mean values of the KW was estimated as:

$$KW = \frac{L_{in} + L_{out}}{2} \; (mm) \tag{1}$$

Dross describes the height of the re-solidified material that adheres to the bottom edge of a cut produced by a thermal process. The dross height (D) was measured using a Starrett-734 digital micrometer with 0.001-mm resolution

Fig. 5 Photographs showing the cutting qualities for the two preliminary tests
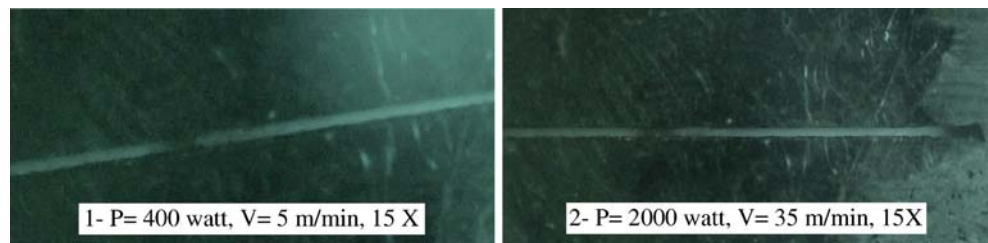
Table 4 Experimental parameters and levels

Input parameters	Symbol	Level				Output parameters
		1	2	3	4	
Laser power (W)	P	800	1,200	1,600	2,000	Kerf width, KW (mm)Dross height, D (mm)Slope, S (°)
Cutting speed (m/min)	V	7.5	15	22.5	30	
Material thickness (mm)	T	1	3	6	10	
Gas pressure (bar)	Pr	3	6	9	16	
Laser mode	M	CW	P1	P2	P3	

The above two experiments exhibit opposite limits of cutting qualities and set the lower and upper bounds for each control parameter. It is safe to say that the allowable range for each control parameter is between the bounds set up by the two experiments, i.e., laser power between 800 and 2,000 W and cutting speed between 7.5 and 30 m/min. During the following matrix experiments, the levels for every control parameter should be specified. With the above-established ranges of control parameters, the maximum, the minimum, and two others in between were chosen for each control factor. Table 3 summarizes the control parameters and their assigned levels.

2.4 Design of experiments

Design of experiments (DOE) is a structured, organized method for determining the relationship between factors which affect the process and the output of that process. The Taguchi technique is a powerful tool for the design of high-

quality systems. Taguchi parameter design can optimize the performance characteristics through the setting of design parameters and reduce the sensitivity of the system performance to the source of variation. In this study, the Taguchi technique with five cutting parameters, namely, laser power, laser speed, material thickness, assistance gas pressure, and laser mode, at four levels were selected. Table 3 summarizes the control parameters and their assigned levels. Table 4 shows the experimental design matrix and experimental results. This table also gives the computed values of the signal-to-noise (S/N) ratio of the kerf width (KW), dross height (D), and slope of cut (S). Taguchi used the S/N ratio as the quality characteristic of choice. The S/N ratio is used as a measurable value instead of the standard deviation because, as the mean decreases, the standard deviation also decreases, and vice versa [25, 26]. By comparing the S/N ratio of the observed values, the optimal combination levels of the cutting parameters were determined. Each experiment is repeated three times to

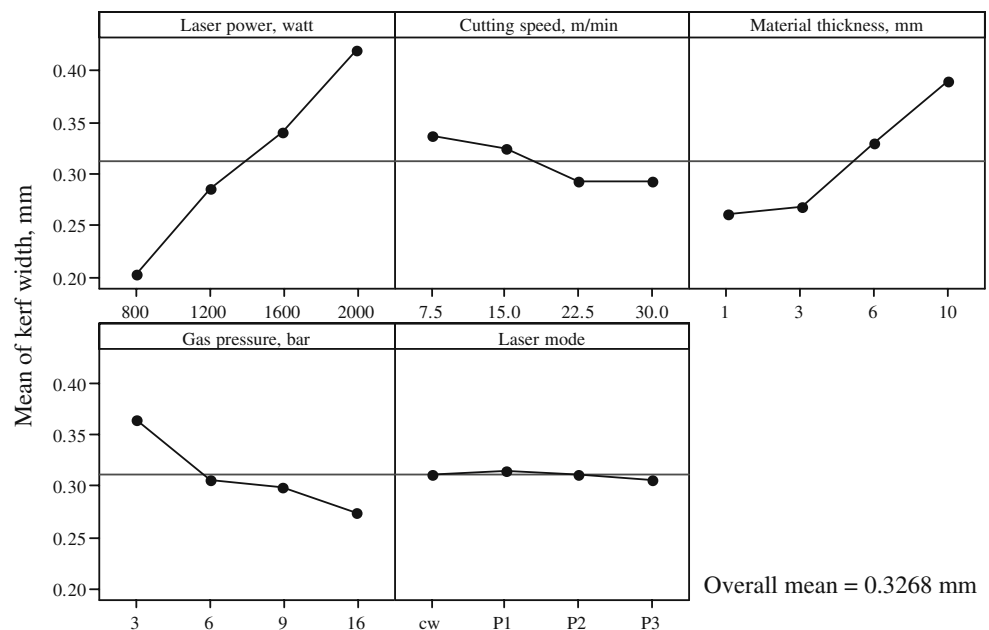**Fig. 6** Main effects plot (data means) for the kerf width

Overall mean = 0.3268 mm

Table 5 L 16 matrix for the experiments and experimental results

Exp. no.	Input parameters					Experimental results					
	P	V	T	Pr	M	KW		D		S	
	W	m/min	mm	bar		mm	η (dB)	mm	η (dB)	°	η (dB)
1	800	7.5	1	3	CW	0.23	12.7654	0.14	19.1721	2.68	−8.5627
2	800	15	3	6	P1	0.19	15.3910	0.14	17.0774	2.62	−8.3660
3	800	22.5	6	9	P2	0.19	14.4249	0.15	16.4782	2.52	−8.0280
4	800	30	10	16	P3	0.22	13.1515	0.17	15.3910	2.39	−7.5680
5	1,200	7.5	3	9	P3	0.25	12.0412	0.26	11.7005	2.66	−8.4976
6	1,200	15	1	16	P2	0.21	13.5556	0.14	17.0774	2.38	−7.4214
7	1,200	22.5	10	3	P1	0.4	7.9588	0.41	7.7443	2.74	−8.7550
8	1,200	30	6	6	CW	0.28	11.0568	0.27	13.1515	2.76	−8.8180
9	1,600	7.5	6	16	P1	0.35	9.1186	0.48	8.4043	2.67	−8.5300
10	1,600	15	10	9	CW	0.42	7.5350	0.51	5.8486	2.87	−9.1576
11	1,600	22.5	1	6	P3	0.26	11.7005	0.25	12.0412	2.59	−8.2660
12	1,600	30	3	3	P2	0.33	9.6297	0.40	9.1186	2.67	−8.5300
13	2,000	7.5	10	6	P2	0.52	3.3498	0.65	3.7417	3.15	−9.9660
14	2,000	15	6	3	P3	0.5	4.7314	0.58	4.7314	3.08	−9.7710
15	2,000	22.5	3	16	CW	0.32	9.8970	0.48	11.0568	2.69	−8.5950
16	2,000	30	1	9	P1	0.34	9.3704	0.34	12.3958	2.60	−8.2995

reduce the influence of the uncontrolled factors (noise factors). The quality values (y_i) of three-repeated numbers are transformed into the S/N ratio (η) via the relation:

$$SB_\eta = -10 \log \left[\frac{1}{3}\right] \sum_{i=1}^{3} y_i^2 \quad (3)$$

where the quality value with smaller-the-better (SB) style has been assumed for all of the cut quality parameters. A control parameter with the largest effect means that it has the most significant influence on the cutting quality. The analysis of variance (ANOVA) is used to discuss the relative importance of all control parameters on the cutting quality and to determine which control parameter has the most significant effect. The predicted value of the S/N ratio

at the optimum parameter levels (η_{opt}) is calculated by using the following formula:

$$\eta_{opt} = \overline{\eta} + \sum_{i=1}^{k} (\eta_{mi} - \overline{\eta}) \quad (4)$$

where k is the number of control parameters, $\overline{\eta}$ is the overall mean value of the 16 experiments, and η_{mi} is the average S/N ratio for the ith control parameter corresponding to the optimum parameter level.

3 Mathematical modeling

The regression models are very promising for practical applications, such as estimating the observed values and

Table 6 Analysis of the kerf width results

Parameter	Average η (KW) by factor level (dB)				Delta	Rank	Contribution %
	1	2	3	4			
P	13.933*	11.153	9.496	10.802	6.191	1	45.78
V	9.901	10.626	10.995*	7.999	1.094	4	10.82
T	11.848*	11.740	9.833	7.179	3.267	2	24.83
Pr	9.094	10.155	10.843	11.431*	2.337	3	17.15
M	10.314	10.460	10.823	10.828*	0.509	5	1.42

*Optimum level
Overall mean=10.58 dB

Fig. 7 Main effects plot (data means) for the dross
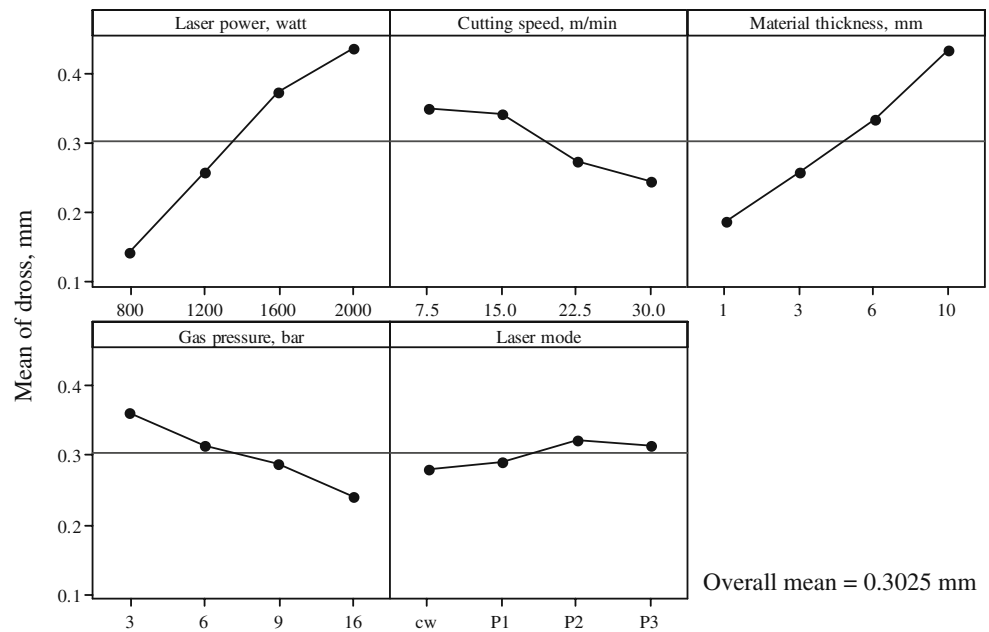
correlated parameters, although the parameters may not be as precise as those produced by the Taguchi method. The models for the quality of cut were developed to evaluate the relationship of laser cutting parameters to the kerf width, dross, and slope of cut. Through these models, any experimental results of kerf width, dross, and slope of cut with any combination of machining parameters can be estimated. The model has been employed on the basis of experimental results. Among several models tested, the exponential model is found to be the best-fit model. The model is implied as several process parameters as follows:

$$y_i = b_0 + \exp\left(b_1 P + b_2 V + b_3 T + b_4 Pr + b_5 M\right) \quad (5)$$

where:

y_i	Quality of cut parameter
b_0–b_5	Constants
P	Laser power (W)
V	Cutting speed (m/min)
T	Material thickness (mm)

Pr Assistance gas pressure (bar)
M Laser mode

The constants b_0–b_5 were calculated using the nonlinear regression analysis method. The kerf width, dross height, and slope of the cut predictor models are:

$$KW = -0.897 + \exp$$
$$(0.00014P - 0.0016V + 0.0122T - 0.005Pr - 0.002M) \quad (6)$$

$$D = -1.007 + \exp(0.0001846P - 0.003293V + 0.0197T$$
$$- 0.00628Pr + 0.0085M) \quad (7)$$

$$S = 1.6181 + \exp\left(0.00025P - 0.0079V + 0.0189T\right.$$
$$\left. - 0.021Pr - 0.0238M\right) \quad (8)$$

The reliability of these models is 0.964%, 0.974%, and 0.952%, respectively.

Table 7 Analysis of dross results

Parameter	Average η (D) by factor level (dB)				Delta	Rank	Contribution %
	1	2	3	4			
P	17.030*	12.418	8.853	7.981	9.048	1	41.26
V	10.755	11.184	11.830	12.514*	1.760	4	8.03
T	15.172*	12.238	10.691	8.181	6.990	2	31.87
Pr	10.192	11.503	11.606	12.982*	2.791	3	12.73
M	12.307*	11.405	11.604	10.966	1.341	5	6.11

*Optimum level
Overall mean=11.571 dB

Fig. 8 Main effects plot (data means) for the slope of cut

Overall mean = 2.692 deg.
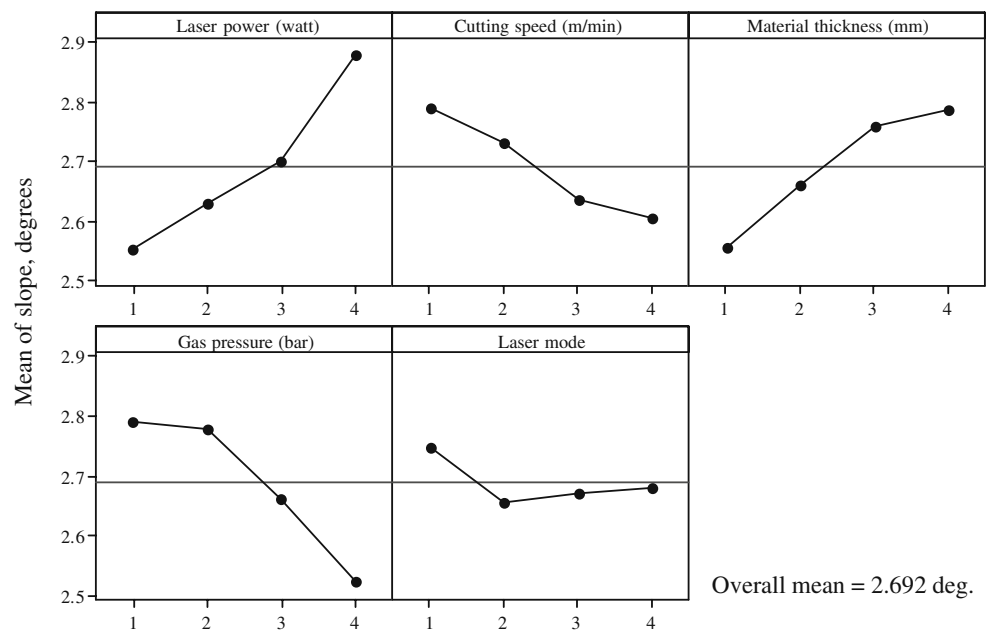
4 Analysis of experimental results and discussion

4.1 Effect of cutting parameters on the kerf width

The kerf widths at the top (L_{in}) and bottom (L_{in}) of the workpiece shown in Fig. 4 are two major parameters to be assessed to evaluate the quality of a laser-cut surface. The kerf width gives an idea of the amount of overcut at the top and the bottom, as well as the taper of the cut surface. With the adopted specific powers (10^5–10^7 W/cm^2), a 'keyhole' plasma column forms, which consists of the decomposition products of the material, and which behaves like a black body for laser radiation. The incident radiation that falls into the keyhole loses some power by absorption and reflection from the plasma, thus, the energy absorbed by the material decreases with the depth along the keyhole. The divergence of the beam beyond the focal plane, which, in the present case, coincides with the top surface of the laminate, is another factor, which leads to a decrease in power density along the keyhole. Furthermore, the energy

absorbed is higher at the center of the beam path due to the higher power density [24]. For the above reasons, the kerf width should be expected to decrease continuously from the top to the bottom of the composite.

Figure 6 represents the main effects plot for the mean value of kerf width against power, speed, material thickness, assistance gas pressure, and laser mode. It can be seen that the kerf width generally increases with increasing laser power and material thickness. This is because of the increases of the incident laser power that is absorbed by the material due to the increasing power level. On the other hand, Fig. 6 reveals a reverse effect for cutting speed on the kerf width due to the decreasing interaction time between the laser beam and the material as a result of the increasing cutting speed. In this case, the rate of energy consumed in cutting reduces, since the laser power remains the same for all cutting speeds. Consequently, sideways burning is minimized and kerf width enlargement is suppressed with increasing cutting speed. Too high a cutting speed may result in a no-cut situation. Furthermore, the kerf width

Table 8 Analysis of the slope of cut results

Parameter	Average η (S) by factor level (dB)				Delta	Rank	Contribution %
	1	2	3	4			
P	−8.131*	−8.373	−8.621	−9.158	1.027	1	29.27
V	−8.889	−8.679	−8.411	−8.304*	0.585	4	16.67
T	−8.137*	−8.497	−8.787	−8.862	0.724	3	20.63
Pr	−8.905	−8.854	−8.496	−8.029*	0.876	2	24.96
M	−8.783	−8.486*	−8.488	−8.526	0.297	5	8.47

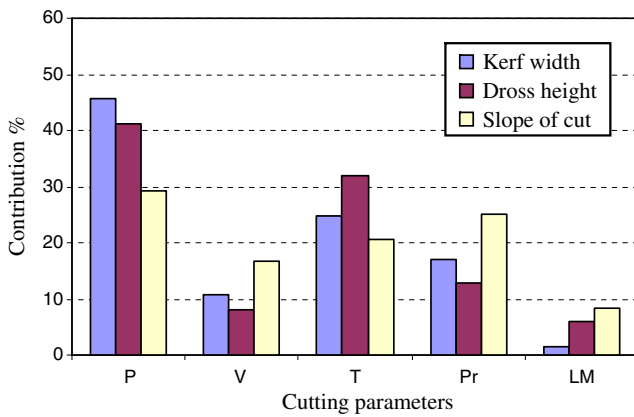*Optimum level
Overall mean=−8.571 dB

Fig. 9 Contribution of cutting parameters on the quality of cut

variation with workpiece thickness becomes considerably significant, which is due to energy diffusion from the kerf wall to solid bulk.

The same trend has been observed for the effect of the assistance gas pressure on the kerf width. The kerf width reduces with increasing assistance gas pressure. This is because the use of assistance gas at a high pressure purges the dross from the kerf site, which, in turn, minimizes the kerf enlargement due to the removal of dross at high temperature remaining in the kerf. A high-pressure assistance gas jet also eliminates the high-temperature oxidation reactions taking place in the kerf during the cutting process (Table 5).

The response table of the S/N ratio for the kerf width (Table 6) indicates that the influence of power has the greatest effect (55.01% contribution) on the kerf width. Hence, the power is the most significant parameter affecting the kerf width (45.78% contribution), followed by the workpiece thickness (24.83% contribution). However, the other parameters have no significant effect (1.42%–17.15% contribution). Based on Table 6, the optimal combination of the parameters for the kerf width could be achieved by using a power of 800 W, thickness of 1 mm, cutting speed of 30 m/min, gas pressure of 16 bar, and the hyper pulse laser mode (P3).

4.2 Effect of cutting parameters on the dross height

Figure 7 shows the main effects of the cutting parameters on the mean of the dross values in the laser cutting process of Kevlar-49. It can be noticed that, with the increase of both power and thickness, the formed dross increases due to the increase of the absorbed laser energy, which increases the molten and resolidified material. It is also clear that the increase of the cutting speed decreases the formed dross due to the decreasing absorption time of the laser energy. The increasing of assistance gas pressure decreases the dross is because of the increased positive effect of the high

Table 9 Optimal parametric settings for KW, D, and S

Quality parameter	P (W)	V (m/min)	T (mm)	Pr (bar)	M
Kerf width	800	30	1	16	P3
Dross height	800	30	1	16	CW
Slope of cut	800	30	1	16	P1

assistance gas pressure for ejecting the molten material from the cutting zone. Furthermore, the laser mode has no significant effects on the dross height.

From Fig. 7 and Table 7 it is clear that the laser power is the most significant parameter affecting the dross height (41.26% contribution), followed by material thickness (31.87% contribution). However, the other factors have no significant effect on the dross height (6.11%–12.73% contribution). Referring to Table 7, the optimal combination of cutting parameters for achieving a lower value of dross is attained by setting the power level at 800 W, cutting speed at 30 m/min, thickness 1 mm, assistance gas pressure at 16 bar, and the continuous wave laser mode (CW).

4.3 Effect of cutting parameters on the slope of cut

The angle of the kerf surface (slope) represents the geometrical accuracy of the machined workpice. Figure 8 displays the main effects of the cutting parameters on the mean value for the slope of cut. As the gas pressure increases, the resultant slope of cut decreases due to the effect of high gas pressure in ejecting the molten materials from the cutting area, while increasing the material thickness causes increasing slope as a result of increasing the laser path in the material. On the contrary, with increasing cutting speed, the slope is decreased because of the wall sides of the cutting width and the difficulties of the molten material removal or blowing out through the kerf obstruct the gas flow. Increasing the laser power increases the resultant slope of cut. This is because, as the laser power increases, the penetration effect increases, which makes the two sides of the cutting edges non-parallel to each other, so the resultant tilting edge of the kerf is larger [14].

Table 8 indicates that the laser power has the greatest effect (29.27% contribution) on the slope of cut. The effect

Table 10 Predicted and experimental values of KW, D, and S at the optimum levels

Quality parameter	Experimental	Predicted	Error %
Kerf width, mm	0.103	0.100	2.90
Dross height, mm	0.101	0.093	7.92
Slope of cut, °	2.060	2.190	6.30

of the material thickness has the second largest effect among the other factors (24.96% contribution), followed by assistance gas pressure (20.63% contribution), cutting speed (16.67% contribution), and then laser mode (8.47% contribution). According to Table 8, the optimal combination of cutting parameters to obtain the lowest slope is attained by setting the power level at 800 W, cutting speed at 30 m/min, material thickness 1 mm, assistance gas pressure at 16 bar, and the first pulsed (gated pulse) laser mode (P1).

Finally, the experimental results (Fig. 9) revealed that the laser power is found to be the most influencing parameter affecting the quality of cut for Kevlar-49 composite, followed by material thickness, assistance gas pressure, and then cutting speed. The laser mode has little influence on the quality of cut.

5 Confirmation experiment

Conducting a confirmation experiment is a crucial final step of Taguchi's parameter design. Its purpose is to confirm that the optimum conditions suggested by the matrix experiment do indeed give the projected improvement. Furthermore, the purpose of the confirmation experiment is to validate the accuracy of the proposed regression models. Conducting tests with the optimal levels combination of the cutting parameters concluded previously entails the confirmation experiments. Table 9 gives the optimal process parametric setting for KW, D, and S. The predicted values of the confirmation tests using Eqs. 6–8 and the experimental observations at the optimum levels of the process parameters are shown in Table 10. It is observed that the predictions based on the purposed regression models is quite close to the experimental observation. The error between the experimental results with the optimum settings and the predicted values for kerf width, dross height, and slope of cut lie within 2.9%, 7.92%, and 6.3%, respectively. Clearly, this confirms the excellent reproducibility of the experimental conclusions.

6 Conclusions

Based on the experimental results, the following conclusions can be drawn:

1. The use of a laser beam appears to be a real alternative for cutting Kevlar-49-reinforced composite under acceptable quality of cut, judged through the kerf width, dross height, and slope of cut, at the optimum process parameter ranges.

2. Laser power is the most significant cutting parameter affecting the investigated quality of cut parameters.

3. The optimum value for the kerf width of 0.103 mm was achieved at laser power 800 W, cutting speed 30 m/min, material thickness 1 mm, and assistance gas pressure 16 bar with hyper pulse laser mode.

4. The minimum dross value of 0.101 mm was obtained at laser power 800 W, cutting speed 30 m/min, thickness 1 mm, and assistance gas pressure 16 bar with continuous wave laser mode.

5. The optimal combination of cutting parameters reduced the slope of cut to 2.06° by setting the power level to 800 W, cutting speed 30 m/min, thickness 10 mm, and assistance gas pressure 16 bar with the gated pulse laser mode.

6. The error between the experimental results at the optimum settings and the predicted values for the kerf width, dross height, and slope of cut lie within 2.9%, 7.92%, and 6.3%, respectively. This confirms excellent reproducibility of the experimental conclusions.

7. The results presented in this paper may become a reference for the CO_2 laser cutting of Kevlar-49 in the aerospace, automotive, and military industries.

References

1. Schwartz MM (1992) Composite materials handbook. McGraw-Hill, New York
2. Ravve A (1995) Principles of polymer chemistry. Plenum Press, New York
3. Al-Sulaiman FA, Al-Nassar YN, Mokheimer EMA (2006) Prediction of the thermal conductivity of the constituents of fiber-reinforced composite laminates: voids effect. J Compos Mater 40(9):797–814
4. Shuaib AN, Al-Sulaiman FA, Hamid F (2004) Machinability of Kevlar 49 composite laminates while using standard TiN coated HSS drills. Mach Sci Technol 8(3):449–467
5. Butt MS, Siddiqui NA, Zafar-uz-Zaman M, Munir A (2003) Study of thermal and mechanical behavior of chemically stabilized phenolic-based composites. In: Proceedings of the 2nd International Bhurban Conference on Applied Sciences and Technology, Islamabad, Pakistan, June 2003, pp 54–60
6. Tandon S, Jain VK, Kumar P, Rajurkar KP (1990) Investigations into machining of composites. Precis Eng 12(4):227–238
7. Chen CC, Cheng W (1991) Material properties and laser cutting of composites. In: Proceedings of the 23rd International SAMPE Technical Conference, November 1991, vol 23, pp 274–287
8. Davim JP, Barricas N, Conceiçãoa M, Oliveirab C (2008) Some experimental studies on CO_2 laser cutting quality of polymeric materials. J Mater Process Technol 198:99–104
9. Yilbas BS (1997) The analysis of CO_2 laser cutting. Proc Inst Mech Eng B J Eng Manuf 211(3):223–232

10. Cenna AA, Mathew P (2002) Analysis and prediction of laser cutting parameters of fibre reinforced plastics (FRP) composite materials. Int J Mach Tools Manuf 42:105–113

11. Zhou BH, Mahdavian SM (2004) Experimental and theoretical analyses of cutting nonmetallic materials by low power CO_2-laser. J Mater Process Technol 146:188–192

12. Bhattacharyya D, Horrigan DPW (1998) A study of hole drilling in Kevlar composites. Compos Sci Technol 58:267–283

13. Mathew J, Goswami GL, Ramakrishnan N, Naik NK (1999) Parametric studies on pulsed Nd:YAG laser cutting of carbon fibre reinforced plastic composites. J Mater Process Technol 89–90:198–203

14. Di Ilio A, Tagliaferri V, Veniali F (1990) Machining parameters and cut quality in laser cutting of aramid fibre reinforced plastics. Mater Manuf Process 5(4):591–608

15. Yilbas BS (2003) Investigation into laser cutting of brush bristles and composite plates. Lasers Eng 13:155–165

16. Al-Sulaiman FA, Yilbas BS, Ahsan M (2006) CO_2 laser cutting of a carbon/carbon multi-lamelled plain-weave structure. J Mater Process Technol 173:345–351

17. Al-Sulaiman FA, Yilbas BS (2005) Laser treatment of a carbon/carbon reinforced composite. Lasers Eng 15(1–2):119–127

18. Al-Sulaiman FA, Yilbas BS, Karakas FC, Ahsan M, Mokheimer EMA (2007) Laser hole cutting in Kevlar: modeling and quality assessment. Int J Adv Manuf Technol (in press) DOI 10.1007/s00170-007-1167-9

19. Hirogaki T, Aoyama E, Inoue H, Ogawa K, Maeda S, Katayama T (2001) Laser drilling of blind via holes in aramid and glass/epoxy composites for multi-layer printed wiring boards. Composites A 32:963–968

20. Di Ilio AM, Tagliaferri V (1989) Thermal damage in laser cutting of (0/90)2s aramid/epoxy laminates. Composites 20(2):115–119

21. Doyle DJ, Kokosa JM (1986) Chemical by-products of laser cutting of Kevlar, polymer preprints, Division of Polymer Chemistry. Am Chem Soc 27(2):206–207

22. DIN standard EN ISO 9013:2000

23. Tani G, Tomesani L, Campana G (2003) Prediction of melt geometry in laser cutting. Appl Surf Sci 208–209:142–147

24. Meijer J (2004) Laser beam machining (LBM), state of the art and new opportunities. J Mater Process Technol 149:2–17

25. Taguchi G (1990) Introduction to quality engineering. Asian Productivity Organization, Tokyo

26. Ross PJ (1989) Taguchi technique for quality engineering, 2nd edn. McGraw-Hill, New York